2018 OCEAN SCIENCES MEETING
11-16 February • Portland, Oregon
#PS44B-2282

Observations of wind-driven internal waves near the buoyancy frequency

E. M. van der Lee[1], F. Cyr[2], M. Buckley[3], L. Umlauf[4], H. van Haren[5]

[1]Leibniz Institute for Baltic Sea Research Warnemünde (IOW), Warnemünde, Germany; [2]Fisheries and Oceans Canada(DFO), Northwest Atlantic Fisheries Centre, St. John's, Canada; [3]Institute of Coastal Research, Helmholtz-Zentrum Geesthacht (HZG), Geesthacht, Germany; [4]Royal Netherlands Institute for Sea Research (NIOZ), Den Burg, the Netherlands

Fisheries and Oceans Canada
Pêches et Océans Canada

Leibniz Institute for Baltic Sea Research Warnemünde

Fonds de recherche sur la nature et les technologies Québec

Context

A high-resolution mooring (ADCP and 150 thermistors vertically separated by 20cm) witnessed the passage of winterstorm Xynthia on the Baltic Sea (early March 2010). Observations suggest that the storm generate both a near-inertial response [van der Lee et al., 2011, JGR 116(C10)] and a much higher frequency response with the generation of internal waves near the buoyancy frequency. We present preliminary results on this last mechanism that is believe to rapidly transfer energy to the permanent pycnocline. This mechanism may enhance exchanges between the anoxic bottom layer and the water above, with consequences for the biogeochemistry of this layer.

Description of the experiment and background conditions

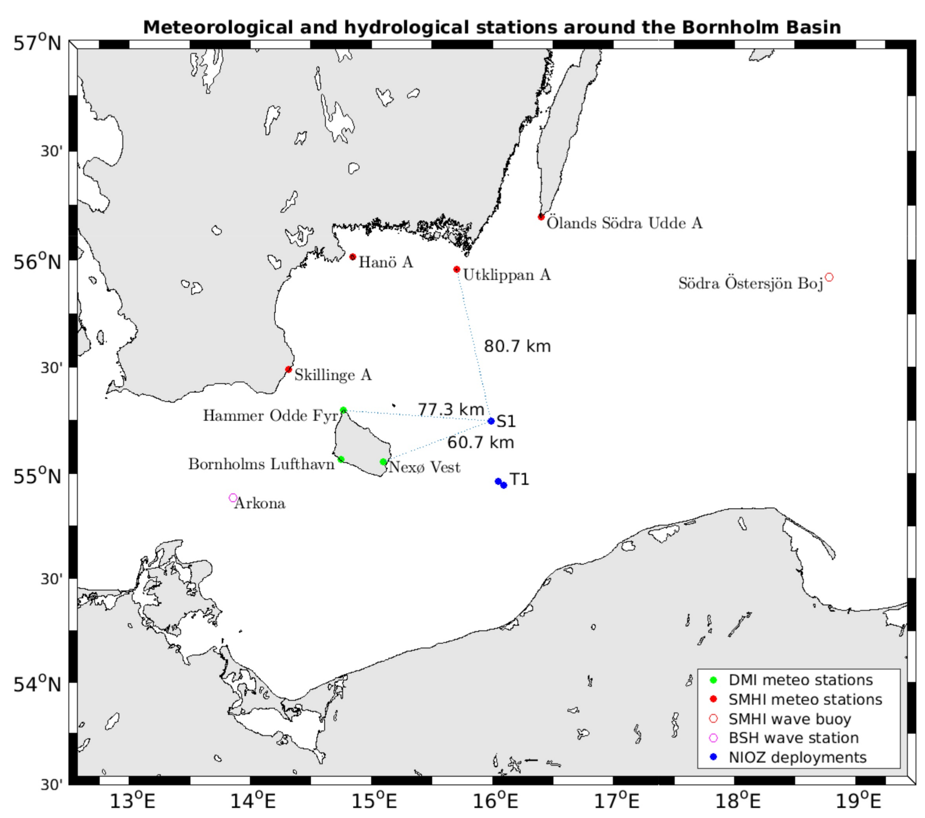

Figure 1. Map of the study area in the Baltic Sea (Bornholm Basin). The mooring was deployed at station S1 between 28 February and 4 March 2010. Data are completed with shipborne microstructure profiler data (MSS90-L). Atmospheric and oceanic weather stations around the site are highlighted.

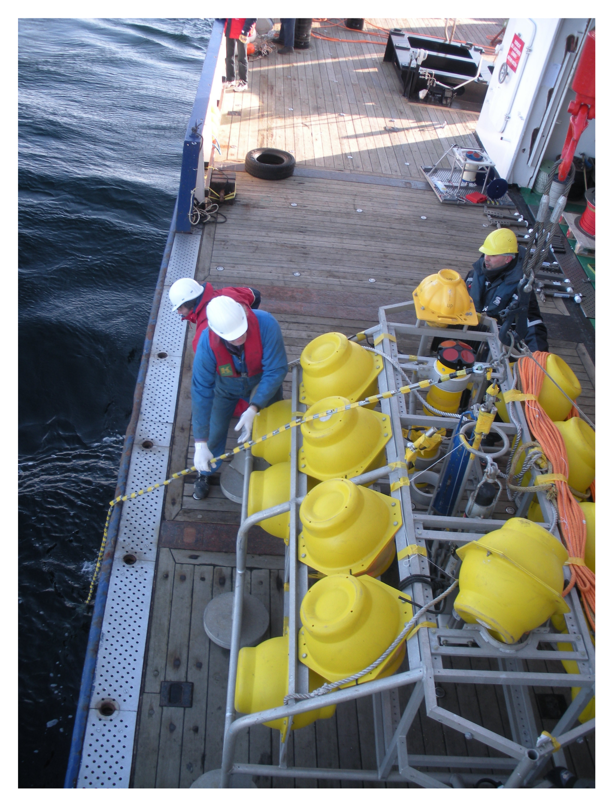

Figure 2. The mooring deployed at S1. Upward looking ADCP on a bottom frame and 150 thermistor equally spaced between 0.1m and 29.9m above bottom (20cm vertical recolution).

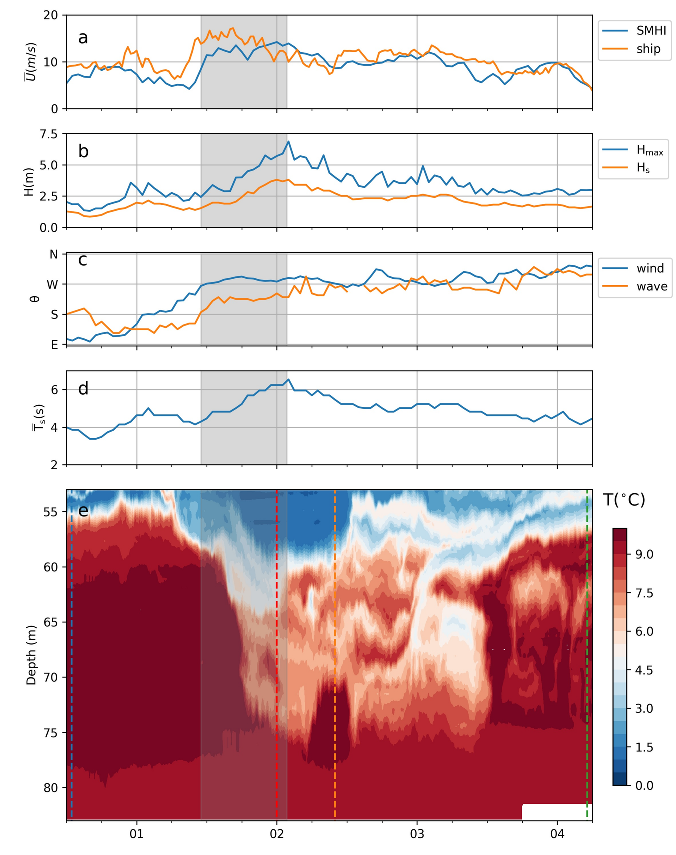

Figure 4. Outlook of the meteorological conditions during the mooring deployment period.
a) Wind velocity measured at SMHI meteo station Utkilppan A (see map Figure 1), as well as from the R/V Alkor meteo station.
b) Maximum (Hmax) and significant (H_s) wave heights
c) Wind and wave direction d) Mean wave period. Wind and wave properties are measured at SMHI meteo station Utklippan A and buoy Södra Östersjön, respectively.
e) Low resolution (10-min time average) temperature field as measured by the mooring for the duration of the deployment.
Shaded time period approximately correspond to the peak wind intensity.

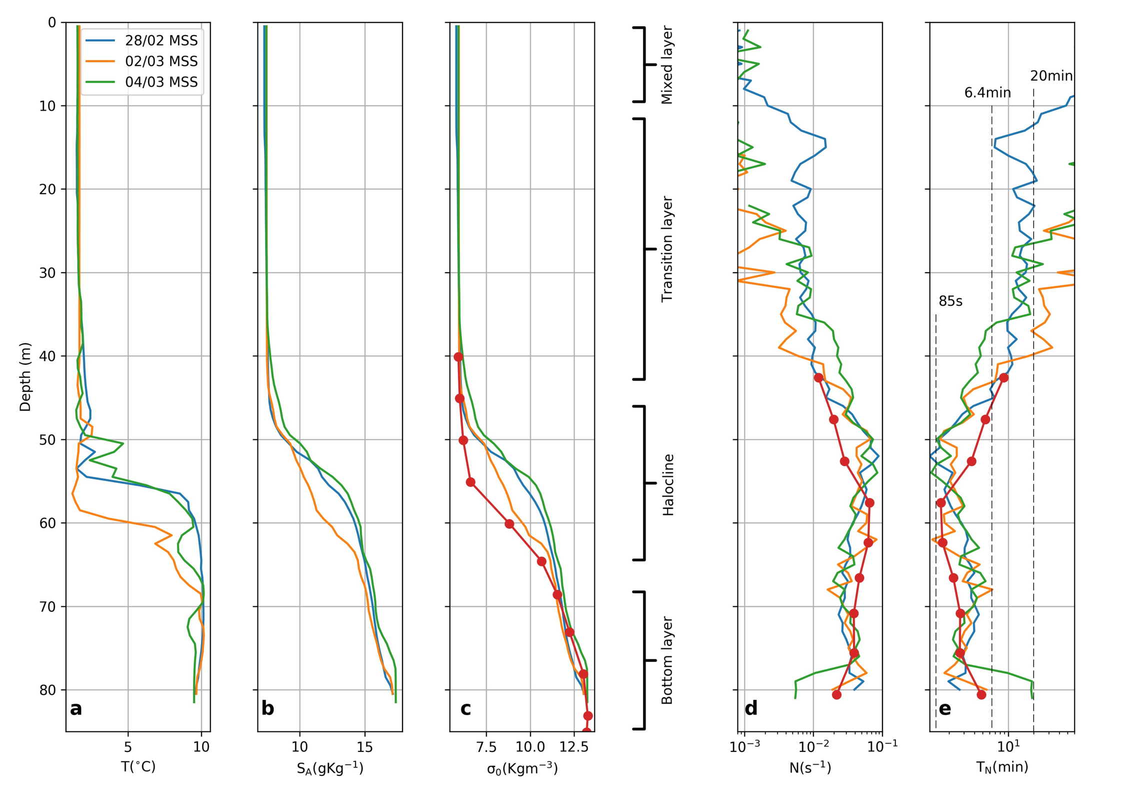

Figure 3. Background oceanographic conditions before, during and after the storm. The weak seasonal thermocline (~15m) is barely visible while the permanent halocline (~55m) isolate the bottom layer from exchange with above.
a) Conservative temperature;
b) Absolute salinity;
c) Density anomaly referenced to surface;
d) Buoyancy frequency squared;
e) Buoyancy period.
While solid lines correspond to MSS casts, the dotted-line corresponds to measurements realized with a moored array of SBE Microcats CTD. The timing of the casts/profiles are identified with corresponding colored dashed lines on Figure 3e.

Water column response to the storm

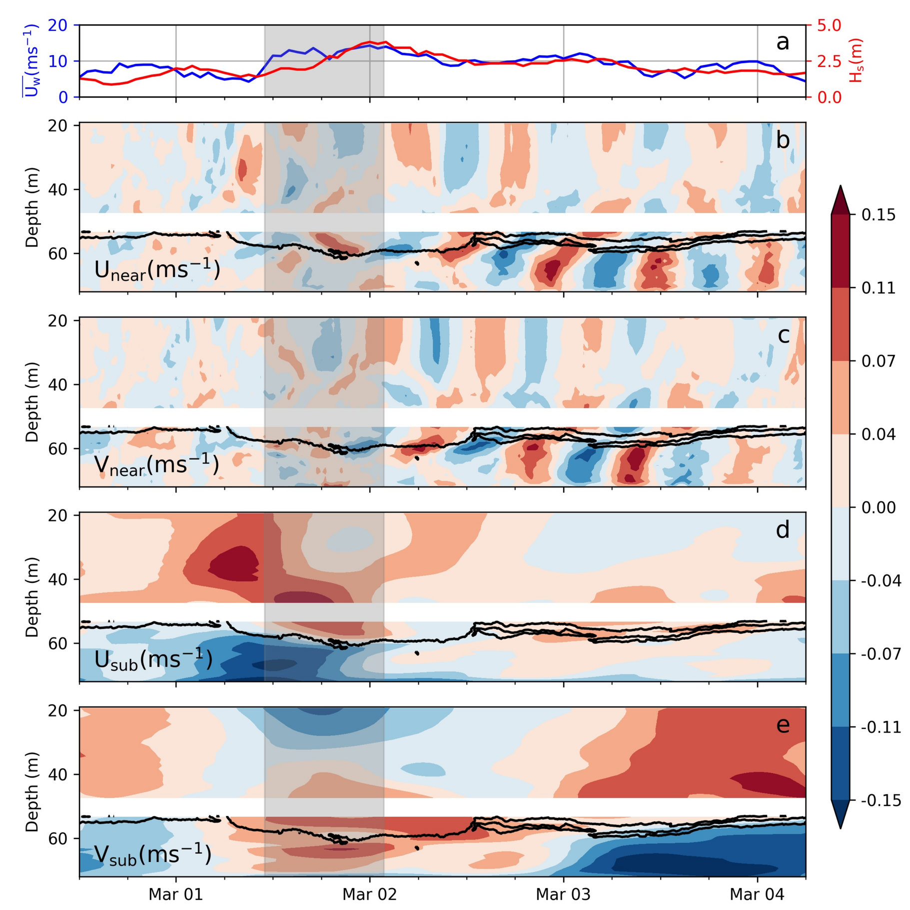

Figure 5. Low-frequency response to wind forcing. a) Hourly mean wind velocity (Uw) and significant wave heights from Figures 3 are reproduced here for reference. b-c) Near-inertial horizontal currents measured by the ADCP. These are obtained after filtering 30-min average currents with a high-pass (20\,h cutoff) Butterworth filter. d-e) Sub-inertial velocities currents measured by the ADCP. These are obtained after subtracting the near-inertial part from the total baroclinic velocities. For reference, isotherm 4ºC is plotted as a black contour.

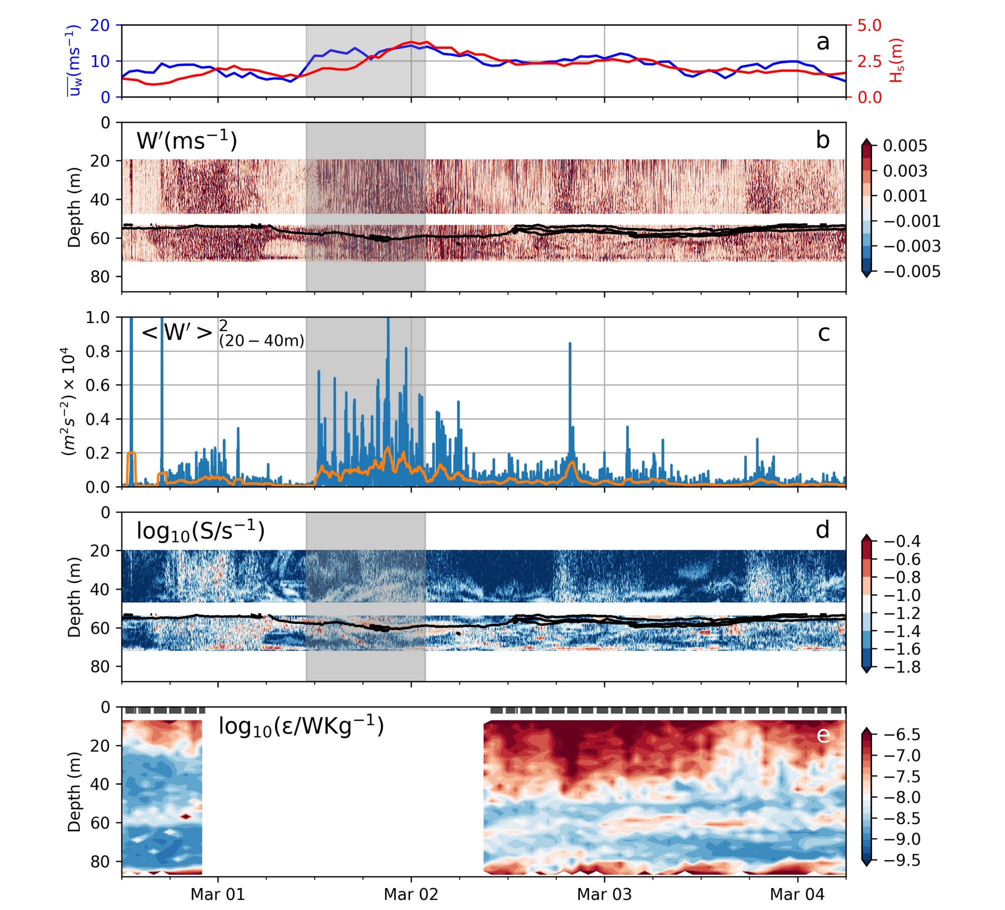

Figure 6. High-frequency response to wind forcing. a) Hourly mean wind velocity (Uw) and significant wave heights from Figure 3 are reproduced here for reference. b) High-pass filtered vertical ADCP velocities (30-min cutoff). c) Square of the vertically averaged velocities of panel b over the range 20-40m (blue) and its 1h moving average smooth (orange) d) Mean horizontal shear from full ADCP measurements. e) Dissipation rates of turbulent kinetic energy averaged in 60 minutes window. Grey tick marks at the top of the panel indicates the location of the 428 casts used for this figure. The black contours in panels b and d is the same as in Figure 4. Shaded time period approximately correspond to the peak wind intensity.

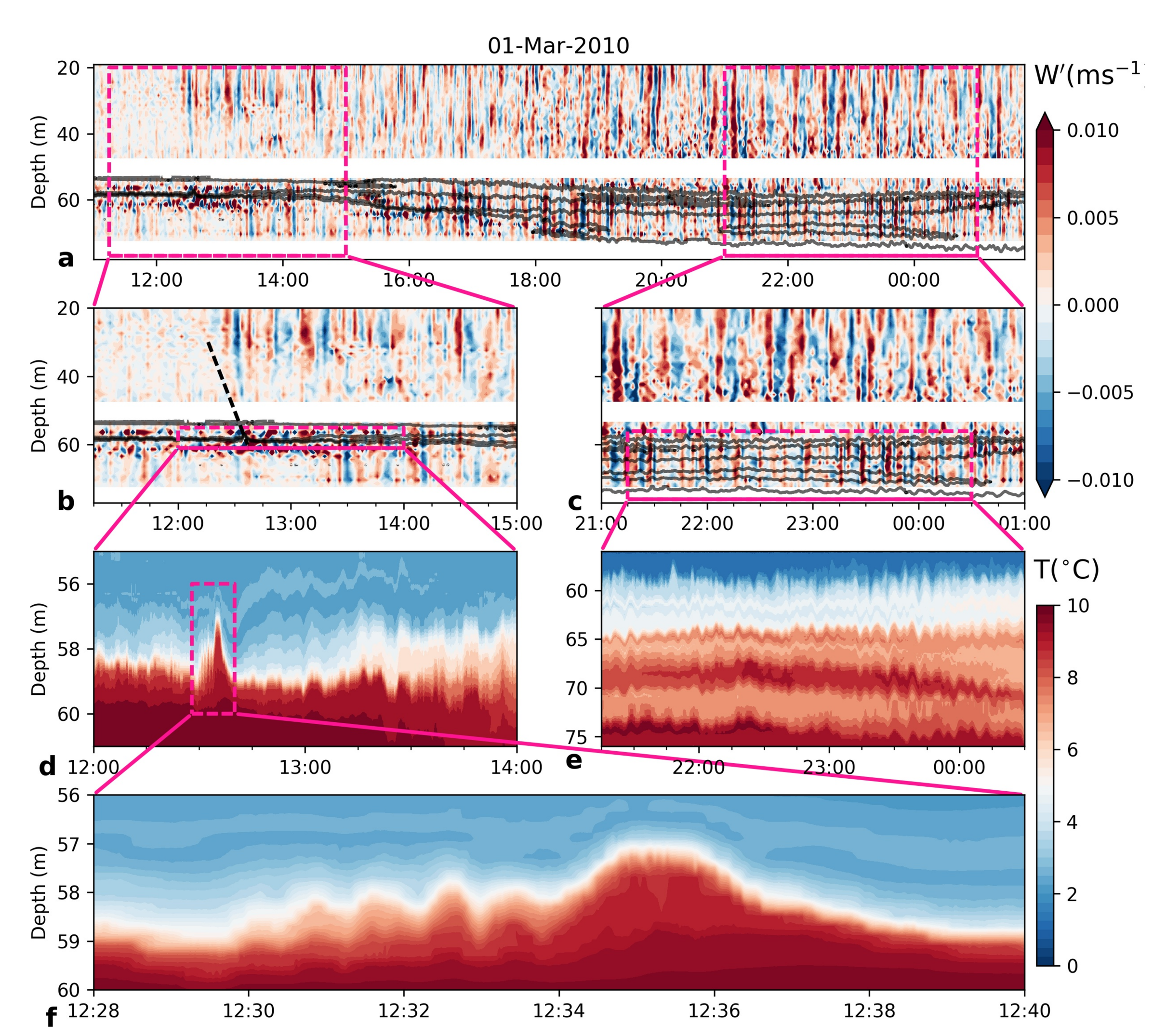

Figure 7. Focus on peak wind intensity. a) Subset of high-pass filtered vertical ADCP velocities (shaded rectangle in Figure 5). Black contours are isotherms [2,4,6,8,10]ºC. b) Enlargement from panel a: onset of high frequency internal waves in the transition layer. c) Enlargement from panel a: Internal waves impinging on the pycnocline. d) Temperature field corresponding to a subset of panel b. e) Temperature field corresponding to a subset of panel c. f) Enlargement from panel d: Large ampplitude internal wave train solitary wave. Note that vertical axis in panels d, e and f are different.

Element of discussion

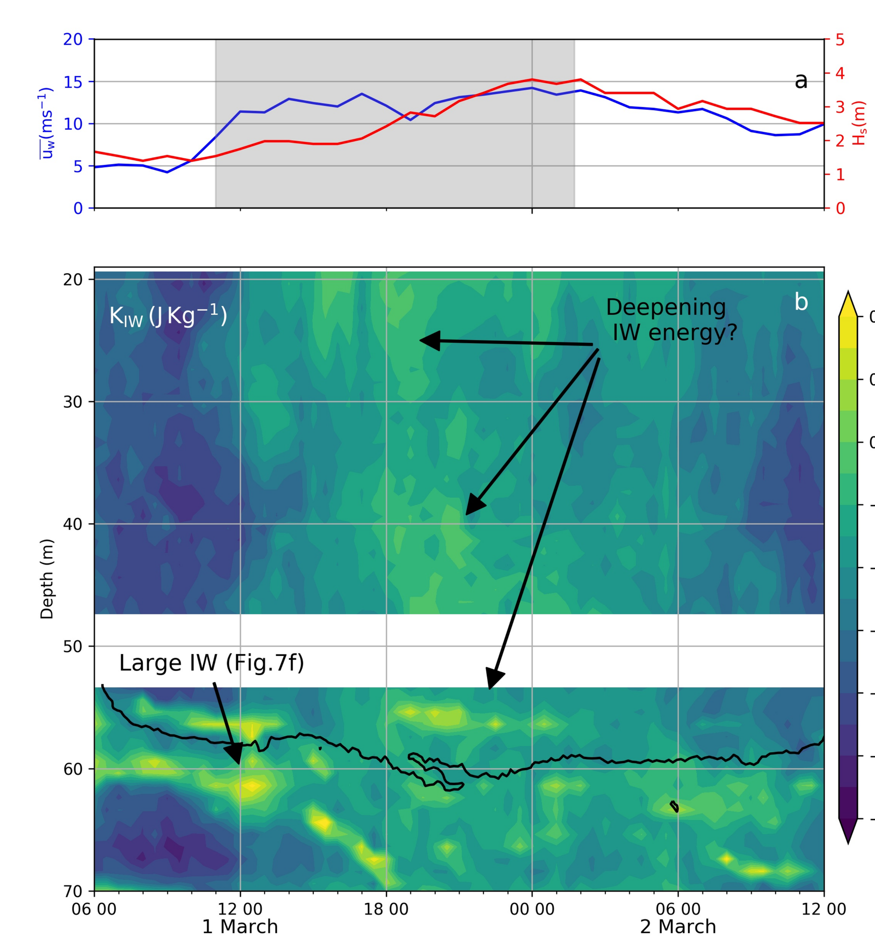

Figure 8. Kinetic energy of high frequency motions in function of time and depth.
a) Hourly mean wind velocity (Uw) and significant wave heights from Figure 3 are reproduced here for reference.
b) Kinetic energy of of high frequency motions calculated as:

$$K_{IW} = 0.5\rho_0(U'^2 + V'^2 + W'^2),$$

where U', V' and W' are the high-pass filtered (30-min cutoff, see Figure 6b for W') and $\rho_0 = 1010\,\mathrm{kg\,m^{-}3}$.

The white horizontal band near 50m has been flagged because of noise created by the floatation devices.

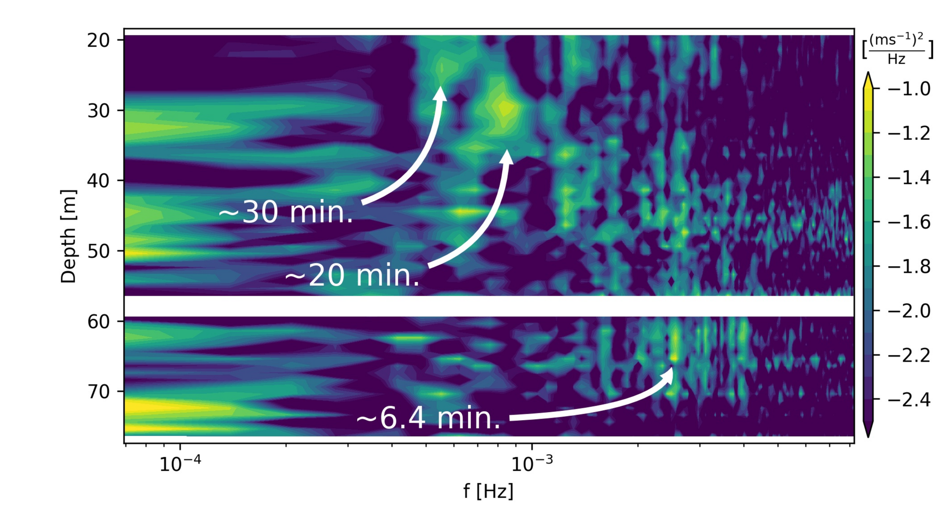

Figure 9. Power Spectra Density contours of the vertical velocities in function of frequency and depth. It shows that vertical oscilations are faster at depth and match the buoyancy period of Figure 3e. Note that the oscilation period in the transition layer (~20 min) is 3 times the one in the pycnocline (~6.4 min).

Bring home message

-> While the original abstract suggested the generation of internal waves by Langmuir circulation, a closer look at the data rather suggests that 2 sets internal waves (IWs) near the buoyancy frequency are present;
-> Ws in the transitional layer are likely generated by surface processes (surface waves, Langmuir, etc.) as their vertical extent deepens with time;
-> IWs riding on the permanent halocline are rather generated by the IWs in the transitional layer impinging on the interface or by the shear generated by near-inertial waves;
-> Preliminary results suggest that the IWs in the transition layer and at the halocline are coupled: the frequency of the former is a fraction of the latter.

Acknowledgements

F. Cyr acknowledge the financial support of both the Fonds de recherche du Québec - Nature Technologies for a post-doc fellowship realized at the NIOZ and the Leibniz Institute for Batic Sea Research Warnemünde (IOW) for a scientific stay at the institute during which this work was initiated.

Questions or comments:

Frederic.Cyr@dfo-mpo.gc.ca

https://cyrf0006.github.io/

Fisheries and Oceans Canada   Pêches et Océans Canada